PERGAMON International Journal of Multiphase Flow 25 (1999) 139–154

International Journal of Multiphase Flow

Particle interaction with the wall surface in two-phase gas–solid particle flow

A.V. Nguyen, C.A.J. Fletcher *

Centre for Advanced Numerical Computation in Engineering and Science (CANCES), The University of New South Wales, Sydney, 2052, Australia

Received 10 September 1997; received in revised form 23 February 1998

Abstract

Solid-particle impact interaction with material wall surfaces is a problem in many multiphase flow industrial devices. This interaction affected by flows around curved surfaces (aerodynamic effects) is analysed in this paper for generic wall geometry and carrier gas flow. The focus of this paper is to quantify the incidence and reflection of small (near-Stokesian) particles. Particle reflection threshold is found, and depends on both particle Stokes number and carrier gas flow near the wall surface. The analytical results are illustrated and compared with the computational results for cylindrical wall surfaces. The boundary layer theory is employed to predict the key model parameter. The analytical prediction agrees well with the computational results.

Keywords: Particle reflection threshold; Particle rebounding distance; Particle-wall interaction; Confined gas-particle flow; CFD simulation; Multiphase flow

1. Introduction

Interest in problem of fluid dynamics of multiphase systems has developed rapidly in recent years. Situations that occur frequently are concerned with the motion of a gas or liquid which contains a distribution of solid particles. Such situations are encountered in numerous industrial applications. One of the important examples is the movement of dusty gas flow in coal combustion equipment and heat exchangers. For better understanding of the mechanism of the erosive wear and the heat transfer through the wall of these devices, the dynamics of

* Corresponding author: Fax: +61 2 9662 7792; E-mail: C.Fletcher@cances.unsw.edu.au..

0301-9322/99/$ - see front matter
PII: S0301-9322(98)00038-X

near-wall gas-particle flow has been the focus of considerable research in the field of multiphase flow.

There are basically two approaches commonly employed in the study of gas-particle flow: Eulerian and Lagrangian formulations. These approaches of modelling gas-particle flow have been reviewed in the literature (e.g. Elghobashi,1994). In the Lagrangian formulation, the motion of individual solid particles is considered, and the particle trajectories are modelled. The gas phase is considered as continuum. In the Eulerian formulation, both gas and particulate flows are treated as continua, and the phases are regarded as two interacting fluids. This approach of modelling gas-particle flow has attracted very strong attention of researchers, since it makes the computation very economical.

However, some fundamental problems have to be addressed in developing Eulerian models. The continuum hypothesis of the particulate phase in Eulerian formulation is validated by Tu and Fletcher (1995a). The results of computational experiments by Tu and Fletcher (1995b) show that the boundary conditions for the particulate phase in Eulerian modelling of gas-particle flow are not constant, and depend on the particle inertia. The ''no-slip'' boundary conditions for the particulate phase is still valid for very low inertia particles, whereas for the particles of higher inertia, a ''slip'' boundary conditions in the Eulerian formulation, however, can arise for the particulate phase. This boundary problem is evidently associated with the particle interaction with wall.

The study of the particle–wall interaction is significant for further fundamental problems involved in Eulerian formulation, such as the particle reflection phenomenon and the drag correction due to reflected particles in wall-dominated multiphase flow. This knowledge will enhance our understanding of two technically-related issues: surface erosion of the wall material by solid particle impact, and heat transfer in coal combustion equipment and heat exchangers. The velocity of the incident particles impacting on the wall surface is needed for predicting the velocity of the reflected particles if the restitution coefficients are known. Modified heat transfer at the wall in combustion equipment and heat exchangers is associated with the velocities of the incident and reflected particles.

Erosion of wall surface material by solid particle impact is affected by a large number of parameters. One group of these is the characteristics of particle motion in the wall-dominated flow, for example, particle incidence angles and particle inertia which is frequently expressed by the particle Stokes number, St. These parameters are associated with the flow of the carrier gas phase near the wall surfaces. In the subsection ''Material versus fluid mechanics aspects of erosion'' of a recent review, Humphrey (1990) stresses the controlling of particle erosion by controlling particle motion in wall-dominated flows. Two characteristic regimes of particle behaviour with regard to the importance of particle–wall impact interaction may be distinguished, based on the superposition between particle inertia and carrier gas flow (Sommerfeld, 1992):

- The motion of relatively small particles is controlled by fluid motion and turbulent dispersion. The influence of the particle–wall interaction is less important since the particles promptly follow the carrier fluid.
- In the case of large particles, their motion is dominated by inertia. Such large particles respond slowly to changes in the carrier flow near the wall surface in confined flows, so their

motion may be considerably influenced by inertia and wall interaction. The particles can maintain their direction of motion for a long time after they rebound off a wall, which could result in the next collision with the opposite wall.

The boundary between these two regimes is, however, not quantitatively established as yet. The motion of particles having a significant inertia is also affected by gravity. At the transition from the first regime to the second regime, we expect that the gravity effect on the particle deviation from the gas streamline is small compared with the aerodynamic effects. In this paper, we investigate the aerodynamic effects due to the change of flows from straight lines. This problem was studied by Laitone (1979), who found that particles never impact with the wall surface if their Stokes number is smaller than one-fourth. Below this threshold, particles follow the carrier fluid in the wall-dominated flow. Besides Laitone, other investigators (e.g. Finnie, 1960; Tilly, 1979) have drawn specific attention to the importance of the "aerodynamic effect" on the particle–wall interaction. These detailed analyses are based on specific geometry of the wall surfaces and inviscid flow of carrier gas. Laitone's analysis is limited by inviscid plane stagnation flow of the carrier gas phase.

In the present report, the behaviour of small particles in interaction with a wall is analytically investigated for generic wall surface shapes and laminar flow of the carrier gas, which is assumed to be viscous in the boundary layer near the wall surface. We know that the behaviour of two-phase solid–gas flow in engineering practice is more complex. Study of such a turbulent flow is difficult to perform by an analytical method and often requires a numerical technique (e.g. Tu and Fletcher, 1995b). However, many solutions to more complex systems often result from an improved qualitative understanding of the single and simple situations. We use the Lagrangian approach of modelling gas–particle flow, since it is a more fundamental procedure to describe the particle–wall interaction process, and can yield the detailed physics of the particle behaviour near the wall. Our analytical results indicate that the particle reflection threshold is determined by, in addition to the particle inertia, the gas phase flow behaviour near the wall surface which, in turn, depends on the local wall surface geometry.

2. Assumptions

The main assumptions implied in this present study are as follows:

- The gas flow is steady. The effect of gravity on particle motion is small compared with the effect of the carrier gas flow so that particles in the bulk phase follow the gas streamlines[1]. Near the wall surface, particles deviate from the gas streamlines and impact on the wall surface. Let this deposition occur at some distance H measured perpendicularly to the wall surface. We assume that the local distances H are small compared with the characteristic

[1] • This requires that the Froude number, Fr, which is defined in the context of this paper by $Fr = (t_p)^2 g/L$, is significantly less than unity. Although we do not specify the smallness of this number we will expect it to be not greater than 0.01.

length of the system, L:

$$\epsilon = H/L \ll 1. \tag{1}$$

- Molecular and surface forces, e.g. van der Waals forces, in the particle–wall interaction are neglected. This assumption is reasonable for the particles of diameter not smaller than 1 μm. For these particles, Brownian motion is negligible. Forces due to pressure gradient, Magnus forces due to rotation, Saffman (lift) forces and Basset forces are not considered. These forces are expected to have a second-order effect compared with the primary effect of aerodynamic drag (Sommerfeld, 1992).
- Particles are spherical and do not break down in their interaction with the wall surface. The wall surface roughness is small compared with the particle size and does not significantly affect the wall–particle collision process.

3. Lagrangian description of particle motion near wall

Under the conditions assumed above, we can write the motion equation of particle near wall in term of its position given by a vector $\mathbf{R}$ as follows:

$$m\frac{\mathrm{d}^2\mathbf{R}}{\mathrm{d}t^2} = 6\pi\eta R_\mathrm{p}\left(\mathbf{W} - \frac{\mathrm{d}\mathbf{R}}{\mathrm{d}t}\right)\cdot f, \tag{2}$$

where m is the particle mass; η is the gas phase viscosity; $\mathbf{W} = \mathbf{W}(\mathbf{R})$ and is the velocity of the gas phase at position $\mathbf{R}$; t is time; R_p is the particle radius.

We define the following characteristic quantities:

1. The characteristic time of the particle motion is the relaxation time, t_p, defined by:

$$t_\mathrm{p} = \frac{2R_\mathrm{p}^2\rho}{9\eta}, \tag{3}$$

   where ρ is the particle density.
2. The characteristic time of the disturbed gas phase flow, t_g, is defined as the ratio of the characteristic length of the system, L, to the undisturbed velocity, W_∞, of the gas phase flow:

$$t_\mathrm{g} = \frac{L}{W_\infty}. \tag{4}$$

   On the basis of these two characteristics, the particle Stokes number is defined by:

$$St = \frac{t_\mathrm{p}}{t_g} = \frac{2R_\mathrm{p}^2 W_\infty\rho}{9L\eta}. \tag{5}$$

   We can scale the dimensional variables in (2) as follows:

$$\mathbf{r} = \mathbf{R}/L, \tag{6}$$

$$\tau = t/t_{\mathrm{p}}, \tag{7}$$

$$\mathbf{w} = \mathbf{W}/W_{\infty}. \tag{8}$$

In (2), f is the friction factor, which defines the deviation of the gas drag on particle from the Stokes law, and is a function of the local particle slip Reynolds number:

$$f = 1 + h[Re_{\mathrm{p}} \cdot |\mathbf{w} - (\mathrm{d}\mathbf{r}/\mathrm{d}\tau)St^{-1}|]. \tag{9}$$

Here, $Re_{\mathrm{p}} = 2R_{\mathrm{p}}W_{\infty}\rho_{\mathrm{gas}}/\eta$ and is the particle Reynolds number based on the gas far-field flow velocity, W_{∞}. The product of this number and the local slip particle velocity is the local particle Reynolds number. If the particle slip Reynolds number significantly exceeds unity, the most frequently used expression for function h on the right-hand side of (9) is given by: $h(x) = 0.15x^{0.687}$ (Schiller and Nauman, 1933). One can see that the deviation of the drag force from the Stokes law is affected either by the particle Reynolds number based on undisturbed gas velocity, or/and the local particle slip velocity. The Reynolds number of small particles is smaller than unity, regardless of their local velocity in wall-dominated motion. For this reason, we assume that $f = 1$ and the particles obey the Stokes drag force law. This assumption should be reasonable for small (near-Stokesian) particles (of the order of 10 μm diameter), which can be observed on the basis of the particle slip velocity near the wall, given in the following sections.

Equation (2) can be converted into dimensionless form by means of the scaled variables as:

$$\frac{\mathrm{d}^2\mathbf{r}}{\mathrm{d}\tau^2} + \frac{\mathrm{d}\mathbf{r}}{\mathrm{d}\tau} - St \cdot \mathbf{w} = 0. \tag{10}$$

The Stokes number given by (5) is an important parameter in the particle–wall interaction analysis. It expresses the influence of the particle inertia on its deviation from the gas phase streamlines, when the gas phase flow is forced to change its direction in a confined space. We suppose that the deviation of the particles from the gas streamlines onto the wall begins at some position $\mathbf{r}_{\mathrm{o}}$. Since the gas flow is assumed to be steady, we have from (10):

$$\left(\frac{\mathrm{d}\mathbf{r}}{\mathrm{d}\tau}\right)_{\mathbf{r}\equiv\mathbf{r}_o} = St \cdot \mathbf{w}_{\mathrm{o}}(\mathbf{r}_{\mathrm{o}}). \tag{11}$$

Let us assume that the particle reaches the wall at position $\mathbf{r}_{\mathrm{s}}$, which is located away from the wall surface by the particle radius. In the particle–wall interaction situation, the difference of the scaled position vectors, $\mathbf{r}_{\mathrm{s}} - \mathbf{r}_{\mathrm{o}}$, of the deposited particles may satisfy the condition:

$$|\mathbf{r}_{\mathrm{s}} - \mathbf{r}_{\mathrm{o}}| \ll 1. \tag{12}$$

Under this condition we may expand the velocity of gas flow near the wall surface into Taylor's series:

$$\mathbf{w} = \mathbf{w}_{\mathrm{s}} + (\mathbf{r} - \mathbf{r}_{\mathrm{s}}) \cdot (T)_{\mathrm{s}} + \cdots, \tag{13}$$

where T is the diagonal tensor of grad($\mathbf{w}$). The subscript "s" describes the value of T calculated at the position away from the wall surface by the particle radius. Inserting (13) into (10), we have:

$$\frac{\mathrm{d}^2\mathbf{r}}{\mathrm{d}\tau^2}+\frac{\mathrm{d}\mathbf{r}}{\mathrm{d}\tau}-(\mathbf{r}-\mathbf{r}_\mathrm{s})\cdot(T)_\mathrm{s}St=\mathbf{w}_\mathrm{s}St. \tag{14}$$

4. Solution

Since particle deposition satisfies (1), the wall-dominated motion of solid particles is a two-dimensional problem, and can be described by using a local (scaled) coordinates (n, l). The coordinate n is normal locally to the wall surface, and l tangent to it in the direction of the gas flow far from the wall surface. The origin of these local coordinates is located at the position where the particle reaches the wall surface, i.e. $\mathbf{r}_\mathrm{s}\equiv 0$. We denote by a the partial derivative of the tangential velocity of gas flow, w_l, with respect to l at the local coordinate origin:

$$a=\left(\frac{\partial w_l}{\partial l}\right)_\mathrm{s}. \tag{15}$$

It follows from the equation of continuity for the gas phase, div($\mathbf{w}$) = 0, that the partial derivative of the gas flow velocity in the normal direction, w_n, with respect to n at the origin is:

$$a=-\left(\frac{\partial w_n}{\partial n}\right)_\mathrm{s}. \tag{16}$$

The parameter a depends on the geometry of the wall surface, and may be positive on some parts of the wall surface. At these locations, the magnitude of the velocity of the incident and reflected particles, and the rates of erosion and heat transfer, are strongly affected. Our analysis will be focused on these cases.

We have from (14):

$$\frac{\mathrm{d}^2\mathbf{n}}{\mathrm{d}\tau^2}+\frac{\mathrm{d}\mathbf{n}}{\mathrm{d}\tau}+\mathbf{n}\cdot St\cdot a=\mathbf{w}_{sn}\cdot St, \tag{17}$$

$$\frac{\mathrm{d}^2\mathbf{l}}{\mathrm{d}\tau^2}+\frac{\mathrm{d}\mathbf{l}}{\mathrm{d}\tau}-\mathbf{l}\cdot St\cdot a=\mathbf{w}_{sl}\cdot St, \tag{18}$$

These differential equations are subjected to the initial conditions given by (11), which can be transformed into $n-l$ coordinates by:

$$\left(\frac{\mathrm{d}\mathbf{n}}{\mathrm{d}\tau}\right)_{\mathbf{n}\equiv\mathbf{n}_\mathrm{o}}+\left(\frac{\mathrm{d}\mathbf{l}}{\mathrm{d}\tau}\right)_{\mathbf{l}\equiv\mathbf{l}_\mathrm{o}}=St\mathbf{w}_\mathrm{o}(\mathbf{n}_\mathrm{o},\ \mathbf{l}_\mathrm{o})=St(\mathbf{w}_{\mathrm{o}n}+\mathbf{w}_{\mathrm{o}l})=St(-a\mathbf{n}_\mathrm{o}+\mathbf{w}_\mathrm{s}+a\mathbf{l}_\mathrm{o}+\cdots). \tag{19}$$

Here, $\mathbf{n}_\mathrm{o}$ and $\mathbf{l}_\mathrm{o}$ are the normal and tangent vectors of $\mathbf{r}_\mathrm{o}$, respectively, and:

$$n_o = \epsilon = \frac{H}{L} \ll 1. \tag{20}$$

The solutions of (17) and (18), subjected to the initial conditions given by (19) when $\tau = 0$, can be written in the generic formulas for particle velocity components in the n- and l-directions as follows:

$$\mathbf{v}_n = \frac{1}{St}\frac{\mathrm{d}\mathbf{n}}{\mathrm{d}\tau} = \mathbf{w}_{on}\left[\cos(\gamma\tau) + \frac{\sin(\gamma\tau)}{2\gamma}\right]\exp\left(-\frac{\tau}{2}\right), \tag{21}$$

$$\mathbf{v}_l = \frac{1}{St}\frac{\mathrm{d}\mathbf{l}}{\mathrm{d}\tau} = \mathbf{w}_{ol}\left[\cos(\beta\tau) + \frac{\sin(\beta\tau)}{2\beta}\right]\exp\left(-\frac{\tau}{2}\right), \tag{22}$$

where the parameters β and γ depend on the particle Stokes number and the local partial gradient of gas velocity near the wall surface:

$$\beta = \frac{\sqrt{1 + 4aSt}}{2}, \tag{23}$$

$$\gamma = \frac{\sqrt{4aSt - 1}}{2}. \tag{24}$$

Unlike parameter β, parameter γ can be zero or complex, and will significantly affect the particle velocity in interaction with the wall surface. If $\gamma = 0$, l'Hospital's rule indicates that the term in square brackets in (21) is equal to $(1 + \tau/2)$. If γ is complex, employing Euler's formula, we can express the particle velocity by (21) in terms of hyperbolic functions. The result is summarised in Table 1.

The change of the particle velocity $\mathbf{v}_n$ with $\mathbf{n}$ and γ is schematically illustrated in Fig. 1. While n is the normal distance to the particle centre, the magnitude of $\mathbf{n} + (\mathbf{w}_{sn}/a)$ gives the normal distance to the wall surface. The ratio of this distance to ϵ $(= n_o)$ is the dimensionless normal distance in the horizontal axis in Fig. 1. The dimensionless velocity in Fig. 1 is expressed by the ratio of w_n/w_{on}. Results given in Fig. 1 show that particles asymptotically approach the wall surface with zero velocity in the direction normal to the wall surface when $St \leq 1/(4a)$. No reflection of the particles can be expected. We can expect that particle reflection can occur if γ is positive. The value $\gamma = 0$ is defined as the critical parameter γ_c, which depends on the critical particle Stokes number, St_c, and the critical value of the local gradient of gas velocity, a_c.

5. Particle rebounding

The rebounding of solid particles after their impact on a wall surface is dictated by the reflected normal velocity. Since we assume that the interaction energy due to surface forces between the colliding particles and the wall surfaces is small compared with the particle kinetic energy, the reflected normal velocity is determined by the incident normal velocity, $\mathbf{v}_{sn}$ and the restitution coefficient in the normal direction, e_n. The normal trajectory of a reflected particle

Table 1
Particle trajectory and velocity in the normal direction, in dependence on its Stokes number and the local gradient of the velocity of the gas phase at the wall surface

Particle Stokes number	Particle trajectory and velocity in the normal direction
$St > \frac{1}{4a}$	$\mathbf{n}(\tau) = -\frac{\mathbf{w}_{sn}}{a} + \mathbf{n}_o\left[\cos(\gamma\tau) + \frac{1-4\gamma^2}{4\gamma}\sin(\gamma\tau)\right]\exp\left(-\frac{\tau}{2}\right)$
	$\mathbf{v}_n(\tau) = \mathbf{w}_{on}\left[\cos(\gamma\tau) + \frac{\sin(\gamma\tau)}{2\gamma}\right]\exp\left(-\frac{\tau}{2}\right)$
$St = \frac{1}{4a}$	$\mathbf{n}(\tau) = -\frac{\mathbf{w}_{sn}}{a} + \mathbf{n}_o\left[1 + \frac{\tau}{4}\right]\exp\left(-\frac{\tau}{2}\right)$
	$\mathbf{v}_n(\tau) = \mathbf{w}_{on}\left[1 + \frac{\tau}{2}\right]\exp\left(-\frac{\tau}{2}\right)$
$St < \frac{1}{4a}$	$\mathbf{n}(\tau) = -\frac{\mathbf{w}_{sn}}{a} + \mathbf{n}_o\left[\cosh(\gamma'\tau) + \frac{1+4\gamma'^2}{4\gamma'}\sinh(\gamma'\tau)\right]\exp\left(-\frac{\tau}{2}\right)$
	$\mathbf{n}_n(\tau) = \mathbf{w}_{on}\left[\cosh(\gamma'\tau) + \frac{\sinh(\gamma'\tau)}{\gamma'}\right]\exp\left(-\frac{\tau}{2}\right);\ \gamma' = \sqrt{-\gamma}$

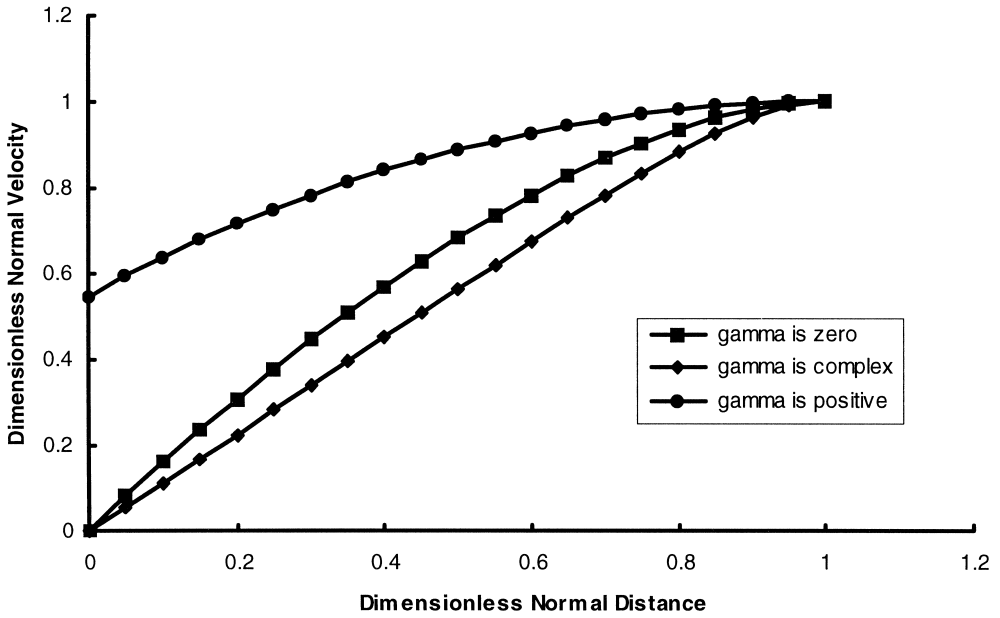

Fig. 1. Normal velocities of particles deposited from gas streamlines in wall-dominated flow. See the text for the definition of the dimensionless coordinates.

can be obtained in the form:

$$\mathbf{n}_{\mathrm{r}}(\tau) = -\frac{\mathbf{w}_{sn}}{a} + [C_1 \cos(\gamma\tau) + C_2 \sin(\gamma\tau)] \exp\left(-\frac{\tau}{2}\right), \tag{25}$$

where C_i ($i = 1, 2$) are the integration constants. Employing the initial conditions: $n_{\mathrm{r}} = 0$ and $\mathrm{d}\mathbf{n}/\mathrm{d}\tau = -e_n \mathbf{v}_{sn} St$ when $\tau = 0$, yields:

$$\mathbf{n}_{\mathrm{r}}(\tau) = -\frac{\mathbf{w}_{sn}}{a} - \mathbf{v}_{sn} e_n St \frac{\sin(\gamma\tau)}{\gamma} \exp\left(-\frac{\tau}{2}\right). \tag{26}$$

The velocity $\mathbf{v}_{sn}$ can be predicted using (21) when $n = 0$. The corresponding time is denoted as τ_{s}. We have:

$$\sin(\gamma\tau_{\mathrm{s}}) = \frac{4\gamma}{4\gamma^2 + 1}, \tag{27}$$

$$\cos(\gamma\tau_{\mathrm{s}}) = \frac{4\gamma^2 - 1}{4\gamma^2 + 1}, \tag{28}$$

$$\mathbf{v}_{sn} = \mathbf{w}_{on} \exp\left(-\frac{\tau_{\mathrm{s}}}{2}\right). \tag{29}$$

Inserting these results into (26) yields:

$$\mathbf{n}_{\mathrm{r}}(\tau) = -\frac{\mathbf{w}_{sn}}{a} + \mathbf{n}_{\mathrm{o}} e_n \frac{4\gamma^2 + 1}{4\gamma} \sin(\gamma\tau) \exp\left(-\frac{\tau + \tau_{\mathrm{s}}}{2}\right). \tag{30}$$

The normal velocity of the reflected particles can be predicted by:

$$\mathbf{v}_{rn} = \frac{1}{St}\frac{\mathrm{d}\mathbf{n}_{\mathrm{r}}}{\mathrm{d}\tau} = -\mathbf{w}_{on} e_n \left[\cos(\gamma\tau) - \frac{\sin(\gamma\tau)}{2\gamma}\right] \exp\left(-\frac{\tau + \tau_{\mathrm{s}}}{2}\right). \tag{31}$$

The change of the normal velocity of the reflected particles with the normal distance in dependence on the dimensionless parameter γ is graphically illustrated in Fig. 2. As expected, no particle reflection occurs when $\gamma = \gamma_{\mathrm{c}} = 0$. If γ is greater than the critical value, the particle rebounding occurs. We conclude at this point that the necessary and sufficient condition for particle reflection threshold to occur is $\gamma = 0$, or equivalently $a_{\mathrm{c}} St_{\mathrm{c}} = 1/4$. Below this threshold the non-slip condition can be applied similarly to the carrier gas flow. A critical point is that the condition of particle reflection threshold is not uniform along the wall surface, since it depends on parameter a. For the inviscid plane stagnation flow, $w_n = -A \cdot n$, where A is a positive constant, we have $a = A$. Setting $A = 1$, we obtain $St_{\mathrm{c}} = 1/4$, which is exactly the same as Laitone's result. Considering the inviscid flow past a cylinder of radius R, we have $w_n = -[1-(1+n)^{-2}] \cos\theta$, where θ is the polar angle measured from the stagnation point. The corresponding a is given by $a = 2(1 + r_{\mathrm{p}})^{-3} \cos\theta$, where r_{p} is the particle radius made dimensionless with the cylinder radius. Since the particle radius is usually smaller than the cylinder radius, the distribution of the critical particle Stokes number over the cylindrical

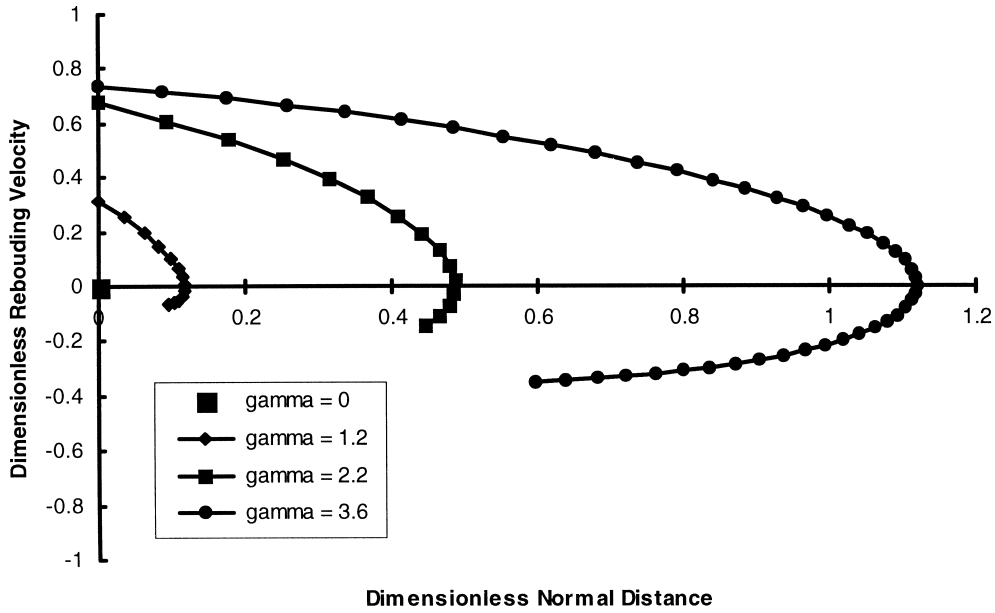

Fig. 2. Normal velocity of a particle reflected off from a wall surface.

surface is described by $St_c = 1/(8\ \cos\theta)$, which at the stagnation point reduces to the well-known value 1/8.

The rebounding distance corresponds to the maximum normal trajectory of the rebounded particles, measured from the wall surface, which can be predicted by:

$$X = e_n \epsilon \frac{4\gamma^2 + 1}{4\gamma} \sin(\gamma \tau_m) \exp\left(- \frac{\tau_m + \tau_s}{2} \right), \tag{32}$$

where τ_m is the time at the maximum normal reflected trajectory, or zero normal reflected velocity. We have:

$$\sin(\gamma \tau_m) = \sqrt{\frac{4\gamma^2}{4\gamma^2 + 1}}, \tag{33}$$

$$\cos(\gamma \tau_m) = \sqrt{\frac{1}{4\gamma^2 + 1}}, \tag{34}$$

Substituting these predictions into (32), we obtain:

$$X = e_n \epsilon \frac{\sqrt{4\gamma^2 + 1}}{2} \exp\left[\frac{\arctan(2\gamma) - \pi}{2\gamma} \right]. \tag{35}$$

This prediction for the rebounding distance, based on the particle Stokes number and the local gradient of gas velocity, is graphically illustrated in Fig. 3.

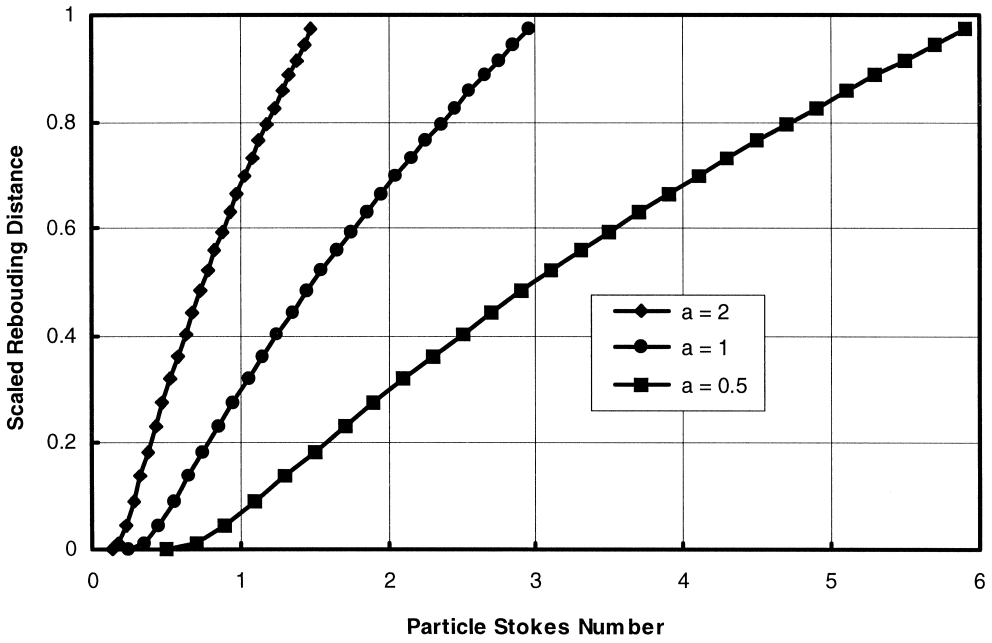

Fig. 3. Rebounding distance in dependence on the particle Stokes number and the local partial derivative of carrier gas velocity, a.

If γ approaches zero, the exponential term in (35) rapidly converges to zero. As a result, the rebounding distance also converges to zero, no reflection occurs. This result is also consistent with the threshold predicted above, on the basis of the incident and reflected particle velocity behaviour.

6. Case study: single cylindrical tube surface

In the previous section, the inviscid gas flow was used to demonstrate the distribution of the particle reflection threshold over the cylindrical wall surface. Since this type of the wall surface frequently occurs in the heat exchangers, we want to focus our attention on this wall surface. Evidently, the inviscid flow corresponds to motion of real carrier gas flow far away from the wall surfaces. The gas motion near the wall surface cannot be described in this limit, because the non-slip boundary condition is not satisfied. The wall-dominated gas flow is viscous, and, therefore, should be better described by the boundary layer approximation.

Since the particle radius is small compared with the cylinder radius, we may expand the carrier gas velocity in the tangential direction into Taylor's series, as follows:

$$(w_l)_s = (w_l)_{wall} + r_p\left(\frac{\partial w_l}{\partial n}\right)_{wall} + \frac{r_p^2}{2}\left(\frac{\partial^2 w_l}{\partial n^2}\right)_{wall} + \cdots \tag{36}$$

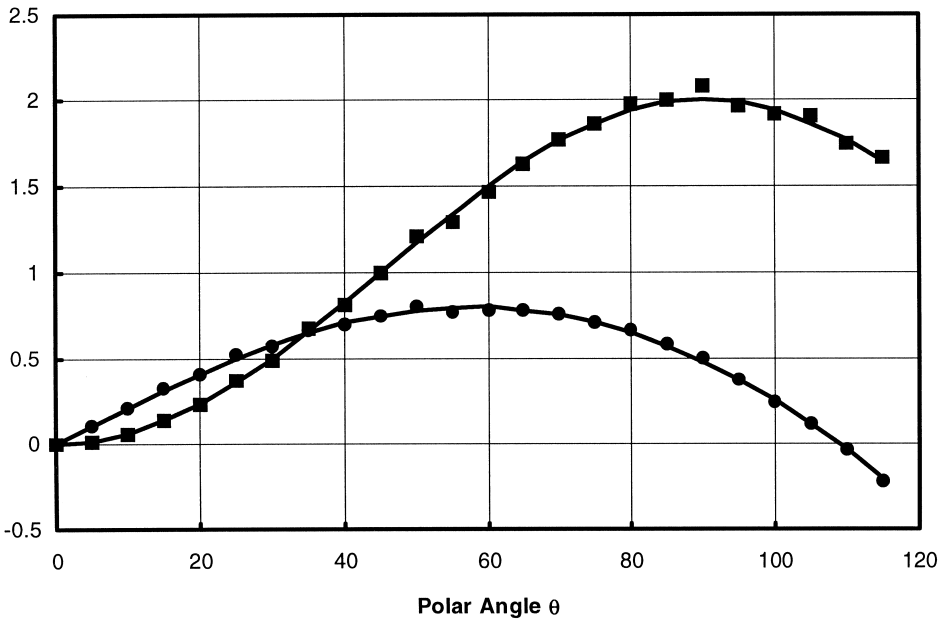

Fig. 4. Distribution of $\xi/(2\sqrt{Re})$ and $(\wp_0-\wp)$ on the surface of a single cylindrical tube. Solid curves describe the boundary layer solutions. Filled circles and squares describe the computational solutions to the Navier–Stokes equations (the mean values for different Reynolds numbers) for $\xi/(2\sqrt{Re})$ and $(\wp_0-\wp)$, respectively.

The first derivative in this equation is equal to the surface vorticity, ξ, of the gas phase flow (made dimensionless by dividing with the characteristic time of the gas phase):

$$\xi = [\mathrm{rot}(\mathbf{w})]_{\mathrm{wall}} = (\partial w_l/\partial n)_{\mathrm{wall}}. \tag{37}$$

The Navier–Stokes equations at the wall surface yield:

$$\left(\frac{\partial^2 w_l}{\partial n^2}\right)_{\mathrm{wall}} = Re\frac{\mathrm{d}\wp}{\mathrm{d}\theta}, \tag{38}$$

where $\wp$ is the surface pressure made dimensionless by dividing with $\rho_{\mathrm{gas}}W_\infty^2/2$; and $Re = 2R_cW_\infty\rho_{\mathrm{gas}}/\eta$, and is the Reynolds number of gas flow past the tube with the radius R_c. Inserting (38) and (37) into (36) one obtains:

$$(w_l)_s = r_p\xi + \frac{1}{2}r_p^2 Re\frac{\mathrm{d}\wp}{\mathrm{d}\theta} + \cdots \tag{39}$$

Both ξ and $\wp$ can be determined by either the computational solution to the Navier–Stokes equations or the boundary layer solution. These two solutions are given for the gas flow of the Reynolds numbers from 2000 to 10^5 in Fig. 4. The details of the computational solution will be described in the next section. The boundary layer solution for the dimensionless surface

vorticity and surface pressure of gas flow past a cylindrical tube can be found as:

$$\xi = 2\sqrt{Re}\left\{\theta f_1 + \sum_{i=1}(-1)^i \frac{(2i+2)}{(2i+1)!}\theta^{2i+1} f_{2i+1}\right\}, \tag{40}$$

$$\wp = \wp_0 - 2\sin^2\theta. \tag{41}$$

Here, f_{2i+1} are the wall surface values of the second derivatives of the functional coefficients in the Blasius series; $\wp_0$ is the surface pressure $\wp$ at the stagnation point. The numerical solution to differential equations for the coefficients of the Blasius series, indicates that the first nine terms of the Blasius series are sufficient to exactly describe the boundary layer flow past a cylindrical tube. The results graphically illustrated in Fig. 4 show a good agreement between the boundary layer solution and the computational solution to the Navier–Stokes equations. Our interest is the gas flow in the windward side of the obstruction where particle reflection occurs. In this case, results in Fig. 4 for surface vorticity can be simply approximated by the following expression:

$$\xi = 2\sqrt{Re}(0.342\sin\theta + 0.595\sin 2\theta - 0.118\sin 3\theta). \tag{42}$$

Inserting (41) and (42) into (39), yields:

$$a = r_p\sqrt{Re}\{0.684\cos\theta + 2.380\cos 2\theta - 0.708\cos 3\theta\} - 2r_p^2 Re\cos 2\theta + \cdots \tag{43}$$

We shall now estimate the error of our prediction given by (43). We can rewrite $r_p^2 Re$ by means of the particle Reynolds number by $r_p Re_p$ and, thus, the order of the cut-off terms in (43) is $O[(r_p Re_p)^{3/2}]$. The order of the particle scaled radius, r_p, and of the particle Reynolds number, Re_p, is 10^{-4} and 1, respectively. Consequently, the order of the cut-off terms in (43) is 10^{-6}. Our prediction given by (43) is sufficiently accurate and can be also written as:

$$a = \sqrt{r_p Re_p}\{0.684\cos\theta + 2.380\cos 2\theta - 0.708\cos 3\theta\} - 2r_p Re_p\cos 2\theta + O[(r_p Re_p)^{3/2}]. \tag{44}$$

7. Comparison with computational results

The commercial CFD code, FLUENT, is used for the simulation of the gas–particle flow past a single cylindrical tube. FLUENT solves the governing equations of the gas flow using a finite-volume method on a non-orthogonal, curvilinear coordinate grid system with a collocated variable arrangement. Pressure/velocity coupling is achieved by the SIMPLEC algorithm, resulting in a set of algebraic equations which are solved using a line-by-line tridiagonal matrix algorithm. The Langrangian formulation of particle motion given by (2) is solved via an advanced Runge–Kutta method to predict particle velocities and trajectories once the gas flow field is obtained. The drag correction factor f is a function of the particle slip Reynolds number of the general form by Morsi and Alexander (1972). The particle trajectory equations are solved by step-wise integration over discrete time steps. During the integration, the gas velocities are calculated from the stored cell-centre velocity using a Taylor expansion.

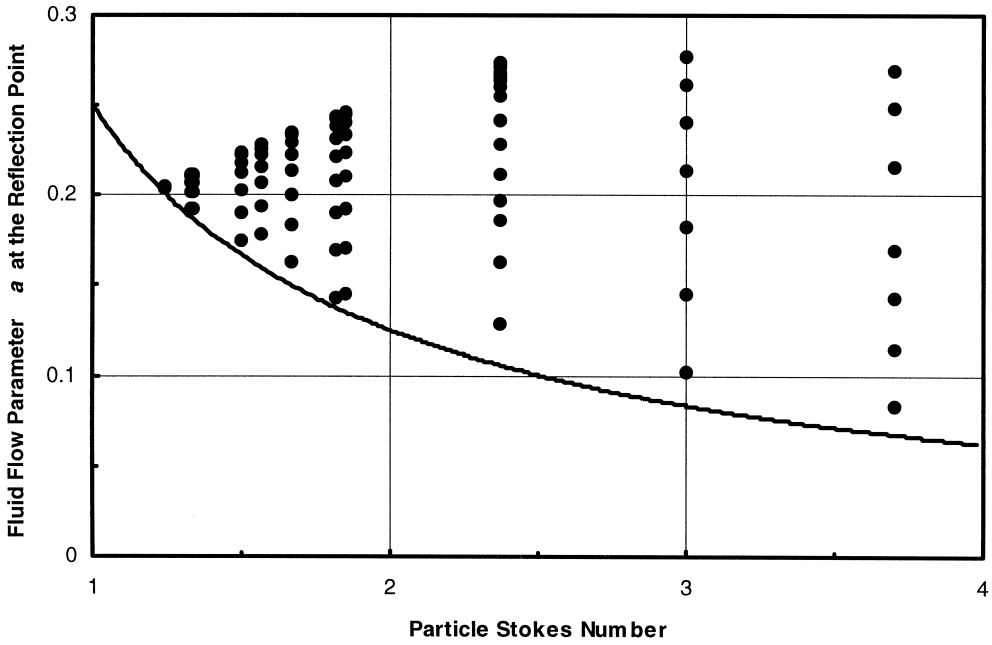

Fig. 5. Threshold of particle reflection as a function of particle Stokes numbers and the local gas flow parameter, a. Prediction is given by solid line ($4St_c a_c = 1$). Points describe the data when the reflection is computationally detected. As expected, no reflection occurs in the domain below the analytically predicted threshold.

Upon striking a wall surface, the particle is forced to rebound according to prescribed restitution coefficients. The restitution coefficients are considered to be 1 in this present paper. Particle fragmentation and particle rotation are not considered. More detailed descriptions of the Eulerian–Langrangian method are provided from the FLUENT User's Guide manual (1996).

Two tube diameters, 0.5 and 1 m are considered in our computational simulation. The gas velocity at the inlet is from 5 to 15 m/s. Two material densities 1500 and 2500 kg/m^3 of solid particles are investigated. The particle diameter changes from 10 to 100 μm. As can be seen later, a good agreement between our prediction and the computational data is observed for these near-Stokesian particles. It may indicate that the assumption $f = 1$ made in our theory may be reasonable for the analysis of the transition of the particle interaction with the obstruction wall from the inertialess regime to the inertial one.

When particles approach the tube wall surface, they may not impact and/or reflect from the wall surface. This is controlled by the particle inertia (the particle Stokes number) and the gas flow, as is shown in our analysis in the previous section. Particles with a small Stokes number do not collide with the wall surface. For an intermediate Stokes number, particles impact the wall surface and are then reflected a certain distance away from the wall, but only at some locations. This is because the impact and the reflection are strongly controlled by the local gas flow at the impact/reflection point. The computational simulation indicates that beyond some polar angle, some particles of a given Stokes number cannot reflect, although they approach the surface. The reflection threshold occurs. In Fig. 5, parameter a expressed by (44) is plotted

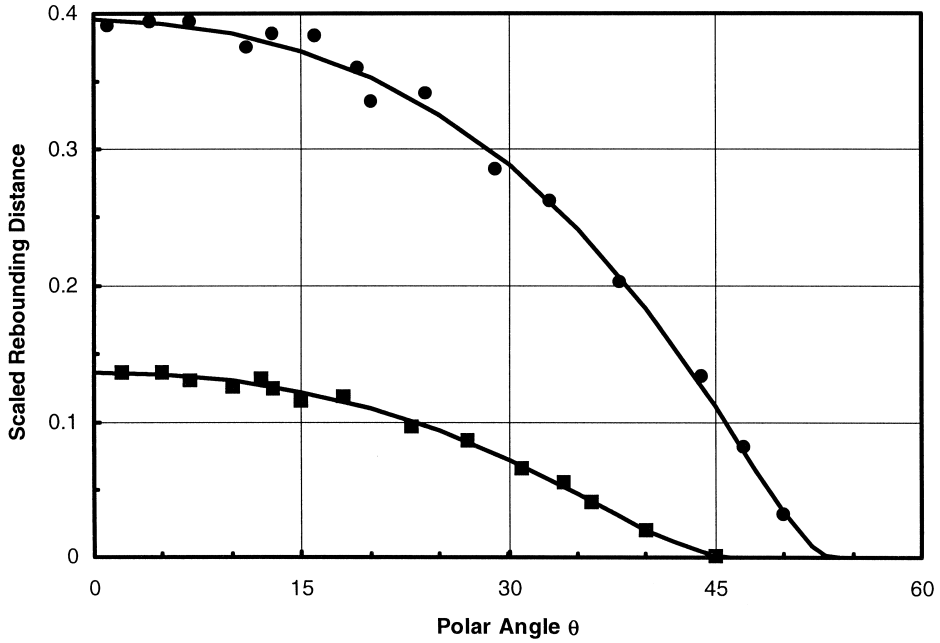

Fig. 6. Comparison between the analytical prediction and the computational results for rebounding distances. The gas velocity at inlet is 10 m/s. The diameter of the single tube is 0.5 m. The diameter of the solid particles is 100 μm (filled circles) and 80 μm (filled squares), respectively. The material density of solid particles is 1500 kg/m^3. Particles of 60 μm diameter impact the tube surface around the stagnation point, but their rebounding distances are significantly small compared with that of, for example, particles of 80 μm diameter.

against the Stokes number for the particles which reflect off from the wall surface. All points lie over the curve of the theoretically predicted threshold. This result substantially differs from Laitone's theory based on inviscid plane stagnation flow, which predicts the threshold by $St_c = 1/4$.

When particle reflection occurs, the particle rebounding and deposition distances (X and ϵ) are determined. The ratios of these distances are plotted against the theoretical prediction given by (35). Parameter a is calculated by (44). Fig. 6 shows an example of the particle–wall rebounding distances, X/ϵ, as a function of the particle Stokes number and the location of particle reflection when the restitution coefficients are assumed to be 1. Good agreement between the prediction and computational results is observed for particle Stokes numbers up to 4. Our theoretical and computational results in Fig. 6 clearly demonstrate that rebounding distances depend not only on the particle Stokes number, but also on local gas flow. It can be seen that the scaled rebounding distance is considerably increased with an increase of the particle diameter (the particle Stokes number). The particles rebound a shorter distance when the polar angle of the impact/reflection points is increased, i.e. when the impact/reflection points move away from the stagnation point and parameter a defined by (15) or (16) becomes smaller.

8. Conclusion

The particle–wall surface interaction is analytically and computationally investigated in this present paper. A universal model for reflection threshold and rebounding distance is obtained. An application of the model to a cylindrical tube surface is illustrated. The boundary layer theory is employed to predict the key parameter of the suggested model. The analytical predictions agree with the computational results and show that impact and reflection of solid particles depends not only on the particle Stokes numbers, but also on the local gas flow at the impact/reflection points. This study illustrates the value of analytical approach for investigating particle motion in the wall-dominated gas–particle flow. Such an approach yields very detailed information about particle velocities in its interaction with a wall surface, which will be useful for predicting surface material erosion. Our results show that the particulate flow near the wall surface is significantly affected by the particle–wall collision process. This fact should be taken into consideration in developing an Eulerian–Eulerian multiphase flow model, which will predict the mean particulate behaviour near the wall surface correctly.

Acknowledgements

The authors gratefully acknowledge the Australian Research Council for the financial support through Grant A9530335.

References

Elghobashi, S., 1994. On predicting particle-laden turbulent flows. Appl. Sci. Res. 52, 309–329.
Finnie, I., 1960. Erosion of surfaces by solid particles. Wear 3, 87–103.
FLUENT User's Guide Manual, 1996. Release 4.4. Fluent Inc., Lebanon, NH.
Humphrey, J.A.C., 1990. Fundamentals of fluid motion in erosion by solid particle impact. Int. J. Heat and Fluid Flow 11, 170–195.
Laitone, J.A., 1979. Aerodynamic effects in the erosion process. Wear 56, 239–246.
Morsi, S.A., Alexander, A.J., 1972. An investigation of particle trajectories in two-phase flow systems. J. Fluid Mech. 55, 193–208.
Schiller, L., Nauman, A.Z., 1933. Über die grundlegenden Berechnungen bei der Schwerkragtaufbereitung. Ver. Deut. Ing. 77, 318–320.
Sommerfeld, M., 1992. Modelling of particle–wall collisions in confined gas–particle flows. Int. J. Multiphase Flow 18, 905–926.
Tilly, G.P. 1979. Erosion caused by impact of solid particles. In: Treatise on Materials Science and Technology. Scott D (Ed.) vol. 13. 287–319. Academic Press, New York.
Tu, J.Y., Fletcher, C.A.J., 1995a. Continuum hypothesis in the computation of gas–solid flows. In: Computational Fluid Dynamics. Leutloff D, Srivastave RC (Eds.) 1–10. Springer, Heidelberg.
Tu, J.Y., Fletcher, C.A.J., 1995b. Numerical computation of turbulent gas–solid particle flows in a 90° bend. AIChE J. 41, 2187–2197.